Available online at www.sciencedirect.com
SCIENCE DIRECT®
Journal of Controlled Release 89 (2003) 499–511
journal of controlled release
www.elsevier.com/locate/jconrel

Humanized docking system for assembly of targeting drug delivery complexes

Marina V. Backer[a,*], Timur I. Gaynutdinov[a], Inna I. Gorshkova[b], Robert J. Crouch[b], Tao Hu[a], Renee Aloise[a], Mohamed Arab[a], Kristen Przekop[a], Joseph M. Backer[a]

[a]*SibTech, Inc., 705 North Mountain Road, Newington, CT 06111, USA*
[b]*Laboratory of Molecular Genetics, National Institute of Child Health and Human Development, NIH, Bethesda, MD 20892, USA*

Received 17 January 2003; accepted 8 March 2003

Abstract

Targeted drug delivery requires 'loading' drugs onto targeting proteins. Traditional technologies for loading drugs rely on chemical conjugation of drugs or drug carriers to targeting proteins. An alternative approach might rely on assembly of targeting complexes using a docking system that includes two components: a 'docking' tag fused to a targeting protein, and a 'payload' module containing an adapter protein for non-covalent binding to the docking tag. We describe here a fully humanized adapter/docking tag system based on non-covalent interaction between two fragments of human pancreatic RNase I. A 15 amino acid long N-terminal fragment of RNase I designed to serve as a docking tag, was fused to the N-terminus of human vascular endothelial growth factor that served as a targeting protein. An 18–125 and an 18–127 amino acid long fragments of RNase I were engineered, expressed and refolded into active conformations to serve as adapter proteins. Interactions between the targeting and adapter proteins were characterized using enzymatic analysis and surface plasmon resonance. Targeting DNA delivery complexes were assembled, characterized by dynamic light scattering, and found to be very effective in receptor-mediated DNA delivery.

Keywords: Targeted delivery; Assembled targeting complexes; Vascular endothelial growth factor; Human RNase; Gene therapy

1. Introduction

Currently, the absolute majority of therapeutic and diagnostic agents is delivered systemically, and their effectiveness depends on differential sensitivity of targeted and bystander cells. The fundamental problem with this approach is that differential sensitivity is not sufficient for more than 99% of drug candidates. As a result, unacceptable side effects are induced, and drug candidates are abandoned during preclinical and clinical development. It is widely recognized that targeted drug delivery to the intended cells might solve these problems. In this approach, the therapeutic effect is based on the enormous ability of targeting molecules to discriminate between targeted and bystander cells.

*Corresponding author. Tel.: +1-860-953-1164; fax: +1-860-953-1317.
E-mail address: mbacker@sibtech.com (M.V. Backer).

0168-3659/03/$ – see front matter
doi:10.1016/S0168-3659(03)00150-0

To exploit full potential of targeted drug delivery it is necessary to have 1) a broad repertoire of targeting proteins; and 2) an efficient technology for loading drugs on these targeting proteins. The repertoire of targeting proteins is growing rapidly due to the genome-based identification of new targeting proteins, generation of diversified single-chain antibody libraries, and production of humanized recombinant monoclonal antibodies. However, lack of efficient technology for loading drugs onto antibodies prevents their widespread use for targeted drug delivery. The available loading technologies are based on chemical conjugation of drugs, drug carriers, or adapters for drug carriers to targeting proteins (see Ref. [1] for review). Chemical modifications of targeting proteins damage their ability to bind to cellular targets, require expensive custom development and yield heterogeneous preparations.

We have recently proposed a new platform technology for modular assembly of targeting complexes [2,3]. This technology avoids chemical modification of targeting proteins by using a standardized docking system that includes two components: a 'docking' tag fused to a targeting protein, and a 'payload' module containing an adapter protein for binding to the docking tag (Fig. 1). Standardized payload modules are pre-made by linking an adapter protein to carriers for therapeutic or diagnostic agents. To obtain a proof-of-principle, we have constructed a docking system based on non-covalent interactions between S-peptide and S-protein fragments of bovine RNase A [2,3]. Payload modules were prepared by conjugating drug carriers to S-protein, and docked to S-peptide fused to vascular endothelial growth factor (VEGF). Assembled targeting complexes delivered their payloads selectively to cells expressing VEGF receptor, VEGFR-2 [2].

To move from proof-of-principle experiments to development of therapeutics, it is necessary to develop a humanized non-immunogenic adapter/docking tag system. Since human RNase I is considered to be the human counterpart of bovine pancreatic RNase A [4,5], we hypothesized that the docking system may be constructed using fragments of RNase I. Our hypothesis was based on the following findings: first, the key N-terminal amino acid residues involved in binding of S-peptide to S-protein in RNase A are conserved in RNase I [6]. Second, the 3-D structures of RNase I and RNase A are remarkably similar [4]. Finally, it was reported that ribonuclease activity of RNase I is reconstituted via interactions between two fragments of RNase I fused to C-termini of single chain antibodies [7].

We report here the development of the first humanized adapter/docking tag system based on non-covalent interactions of two fragments of RNase I. To achieve this goal we engineered, expressed, and refolded an 18–125-aa and an 18–127-aa fragments of RNase I into functionally active conformations. A 1–15-aa fragment of RNase I was fused to N-terminus of human $VEGF_{121}$ as a docking tag creating a protein named Hu-VEGF. Hu-VEGF-driven DNA delivery complexes based on the humanized docking system were found to be very effective in VEGFR-2 mediated DNA delivery.

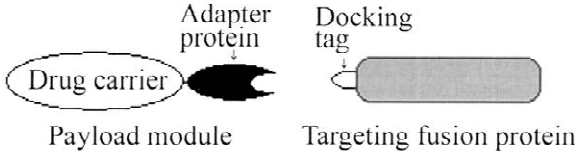

Fig. 1. Modular assembly of a molecular drug delivery complex is based on non-covalent interaction of an adapter protein and a docking tag.

2. Materials and methods

2.1. Construction of pET29/Hu-tag vector

The pET-29a(+) bacterial expression vector (Novagen, Madison, WI) was cut with *Nde*I and *Kpn*I, and gel purified to remove a DNA fragment encoding bovine S-peptide. To reconstitute a DNA fragment encoding Hu-peptide (15 N-terminal amino acids of human RNase I), two single-stranded DNA fragments (synthesized by GeneLink, Thornwood, NY) were mixed in equimolar concentrations and annealed at room temperature for 10 min. One fragment, 5′-TATGAAAGAATCTCGAGCTAAAA-AATTTCAACGTCAACACATGGACTCTGGTAC, corresponded to the 'sense' DNA strand, and the other one, 5′-CAGAGTCCATGTGTTGACGTTGA-AATTTTTTAGCTCGAGATTCTTTCA, complemented the 'sense' DNA strand. After annealing, the

fragments created overhangs compatible with *Nde*I, immediately upstream of the first Hu-peptide codon, and with *Kpn*I, downstream of the last Hu-peptide codon. The annealed DNA fragment was ligated into *Nde*I and *Kpn*I sites of the pET-29a(+) vector. The resulted vector containing the 15-aa Hu-peptide (Hu-tag), a 9-aa linker with a thrombin digestion site, and the MCS of the parental vector, was confirmed by sequencing and designated pET29/Hu-tag.

2.2. Construction of VEGF fusion protein

The pLen-121 plasmid containing the precursor for the 121-amino acid residue of human VEGF was kindly provided by Dr J. Abraham (Scios Nova, Inc., Mountain View, CA). The $VEGF_{121}$ coding sequence was amplified by PCR from the pLen-121 plasmid using a sense primer 5′-CACAAG*CCATGG*CAC-CCATGGCAGAAGGAGGA and an antisense primer 5′-ACTAC*CCATGG*TCACCGCCTCGGCT-TGTCAC, both primers contained *Nco*I restriction sites (italic). The gel purified PCR fragment was cloned in the pET29/Hu-tag in *Nco*I site. The clones with correct VEGF orientation were selected by PCR using a T7-based sense primer.

2.3. Construction of human RNase I fragments

The pET-HP plasmid encoding 1-127 amino acids of RNase I was a generous gift of Dr G. D'Alessio (Napoli Federico II University, Naples, Italy). DNA encoding five RNase I fragments were amplified by PCR from the pET-HP plasmid with sense primers introducing ATG codon immediately upstream of the coding sequences (Table 1). An antisense primer 5′ - **TCA** TTCAACAGACGCGTCGAAATGAACC - GG introduced a stop-codon (bolded) immediately downstream of the ^{125}glu codon. The gel purified PCR fragments were ligated separately into pETBlue-1 vector (Blunt-end ligation kit, Novagen) according to manufacturer's instructions. All constructs were tested for protein expression in *Esherichia coli* strain Tuner(DE3)pLacI (Novagen) according to manufacturer's instructions. To increase protein yield, DNA encoding the 18–125aa RNase I fragment with the ^{19}pro→ala, ^{20}ser→ala substitutions was sub-cloned in pET29a(+). The DNA fragment was amplified by PCR using a sense primer 5′-CAC-AAGCATATGAGCGCTGCCTCTTCTTCTACG introducing *Nde*I site, and an antisense primer 5′-TAC-GGTACCTCAAGAGTCTTCAA CAG ACGCGTCG introducing ^{126}asp and ^{127}ser codons, stop-codon, and *Kpn*I site. The gel-purified DNA fragment was cloned into *Nde*I and *Kpn*I sites of pET29a(+). The resulting DNA constructs were confirmed by sequencing.

2.4. Protein expression

The 18–127 HuS(^{19}pro→ala, ^{20}ser→ala) fragment of RNase I designated $^{18-127}$HuS, Hu-tagged $VEGF_{121}$ designated Hu-VEGF, and human RNase I were expressed in *Esherichia coli* strain BL21(DE3) (Novagen) grown in CircleGrow medium (Q-Biogen, Carlsbad, CA). The expression was induced by 1 mM IPTG (Life Technologies, Rockville, MD) at the optical density of 0.5–0.7 unit at 600 nm. After induction, the cultures were grown for 2 h at 37 °C with shaking at 250–280 rev./min; then harvested by centrifugation for 15 min at 5000×*g*. Inclusion bodies were extensively washed using a combination of BugBuster reagent (Novagen), CelLytic B (Sigma, St. Louis, MO), and HisBind buffer (Novagen) as described in Ref. [8], and then solubilized by sonication in a buffer containing 8 M urea, 20 mM Tris–HCl, 100 mM NaCl, pH 8.0. The $^{18-125}$HuS(^{19}pro→ala, ^{20}ser→ala) fragment of RNase I designated $^{18-125}$HuS was expressed in *E. coli* strain OrigamiB(DE3)pLacI (Novagen) as described for the recombinant bovine S-protein [8], except that the IPTG-induced culture was grown overnight (16–18 h) at 37 °C. S-tagged VEGF, the human $VEGF_{121}$ with an N-terminal bovine S-peptide, was expressed as described in Ref. [2].

2.5. Protein refolding and purification

The HuS concentration in solubilized inclusion body fraction was determined by RP HPLC on C_{18} Waters Nova-Pack 5 μm column (150×3.9 mm) with elution at 0.75 ml/min with 0.1% TFA (v/v) and a linear gradient of acetonitrile (5–50% over 20 min). The concentration was calculated using 216-nm integral absorption in HPLC profiles. Synthetic Hu-peptide (custom synthesized by GeneMed, San Francisco, CA) was added to solubilized inclusion

bodies at the molar Hu-peptide to HuS ratio of 2:1. The HuS/Hu-peptide mixture was refolded in a redox buffer containing 100 mM Tris–Acetate, 100 mM NaCl, 0.5 M arginine, 1 mM glutathione (GSH, Novagen), 0.4 mM oxidized glutathione (GSSG, Novagen), pH 8.6, and then purified by a combination of ion-exchange chromatography and RP HPLC as described for refolding and purification of recombinant bovine S-protein [8]. Hu-VEGF and RNase I were refolded from solubilized inclusion bodies by a two-step dialysis as follows: first, 20 h against 20 V of 20 mM Tris–HCl, 2 M urea, 0.5 M arginine, 1 mM glutathione (Novagen), 0.4 mM oxidized glutathione (Novagen), pH 8.0; then 24 h against 100 V of 20 mM Tris–HCl pH 8.0. RNase I was found to be >95% pure by SDS–PAGE, and was used for experiments without further purification. Misfolded monomers of Hu-VEGF were removed from protein preparations by passing them through HiTrap Q Fast Flow sepharose (1-ml pre-packed columns, Amersham). Concentrations of all recombinant proteins were determined by RP HPLC as described above for HuS.

2.6. Cells

HEK293 human transformed embryonic kidney cells (CRL-1573) were obtained from American Type Culture Collection (Rockville, MD). HEK293 parental cells and 293/KDR cells expressing 2.5×10^6 VEGFR-2/cell (developed as described in Ref. [9]) were grown in DMEM with 10% FBS, 2 mM L-glutamine and antibiotics at 37 °C, 5% CO_2.

2.7. Immunoprecipitation

293/KDR cells were plated on 6-well plates, 0.5–1 million cells per well. Then 20 h later, cells were lysed in ice-cold IP buffer (10 mM Tris–HCl pH 7.5 150 mM NaCl, 1% Triton X-100, 0.5% NP-40, 1 mM EDTA, protease inhibitors) for 30 min at 4 °C, and clarified by centrifugation at $10\,000\times g$ for 5 min. Varying amounts of Hu-VEGF were mixed with clarified cell lysates, incubated for 1 h at 4 °C, and then absorbed from the solution on S-protein agarose (Novagen) for 1 h at 4 °C. Alternatively, Hu-VEGF was first pre-absorbed on S-protein agarose for 1 h at 4 °C, washed twice with IP buffer; and then added to clarified cell lysates, incubated for 1 h at 4 °C, and then pelleted again. In both experimental settings, non-specific cellular proteins were removed from the final S-protein agarose pellets by extensive washing with IP buffer. Binding of cellular VEGFR-2 to Hu-VEGF was analyzed by Western blotting using Flk-1 (A-3) mouse monoclonal antibody sc-6251 (Santa Cruz Biothechnology, Santa Cruz, CA) diluted 1:200, followed by anti-mouse IgG:HRPO conjugate (Amersham Biosciences, Picsataway, NJ).

2.8. HuS/Hu-tag binding assay

The equilibrium dissociation constant (K_D) values for HuS/Hu-VEGF and HuS/Hu-peptide complexes were determined as described [8]. Briefly, HuS at final concentrations of 0.2, 0.4, or 0.6 nM was mixed with varying amounts of Hu-VEGF or Hu-peptide in a buffer containing 20 mM Tris–HCl, 100 mM NaCl, pH 7.5, 0.1 mg/ml poly C (Sigma). After 5-min incubations at room temperature, the reactions were stopped by addition of ice-cold TCA (final of 2.5% v/v), incubated on ice for 5 min, and centrifuged for 10 min at $14\,000\times g$ at room temperature. Activities of the reconstituted ribonucleases were measured by absorbance of the supernatants at 280 nm. One optical unit of acid-soluble material released from poly C incubated with reconstituted ribonuclease was defined as one relative unit of ribonuclease activity. Calculations of the K_D values were performed assuming that the initial rate of the hydrolysis is proportional to the concentration of reconstituted ribonuclease. DYNAFIT software was used for the global fitting with numeric iteration and calculation of the K_D values [10].

2.9. Ribonuclease activity assay

Enzymatic activities of HuS/Hu-peptide complexes, bovine RNase A (Sigma), and human recombinant RNase I were determined in the original and a modified Kunitz's assays [11,12]. In the original Kunitz's assay, a reaction buffer contained 50 mM NaOAc at pH 5.0 with 0.05% (w/v) yeast RNA (Sigma) as a substrate, and the absorbance of the reaction mixtures at 300 nm was recorded at 25 °C as a function of time. In a modified Kunitz assay, a reaction buffer contained 10 mM Tris–HCl at pH

7.5, 50 mM NaCl, with 50 μg/ml poly C (Sigma), and the absorbance was recorded at 260 nm at 25 °C. For testing activities of HuS/Hu-peptide complexes, HuS was added to the reaction buffers supplemented with a 35-fold molar excess of synthetic Hu-peptide. One unit of enzymatic activity was defined as the amount of enzyme that caused a change in A_{300} or A_{260} per min equal to the change generated by the complete transformation of the substrate under the assay conditions.

2.10. Surface plasmon resonance (SPR) analysis

All experiments were performed in the Biacore 1000 system at 25 °C. CM-5 sensor chips with a carboxymethylated dextran matrix, NHS, EDC and P20 surfactant were from BIACORE AB (Uppsala, Sweden). Bovine S-protein or HuS was immobilized on CM-5 chip surface by amine coupling through a slightly modified procedure described in Ref. [13]. Briefly, the surfaces were activated with mixture NHS/EDC according to manufacturer's instructions, treated with 10 μg/ml protein in 10 mM NaOAc at pH 6.8 to the immobilization level corresponding to the baseline increase between 300 and 400 RU, and 'neutralized' with 1 M ethylenediamine pH 8.5. After protein immobilization, the surface was washed with 0.5% SDS mimicking the regeneration step for removing of non-covalently binding proteins. To observe binding, 10 μl of Hu-VEGF or S-tagged VEGF at varying concentrations in TBS buffer (25 mM Tris pH 7.5, 100 mM NaCl, 5 mM EDTA, 0.005% P20) were successively injected at a flow rate of 2 μl/min over the surface using the KINJECT command defining association time of 5 min and dissociation time of 10 min. After each round of injection, bound protein was completely removed by two passages of 10 μl 0.5% SDS followed by TBS running buffer at a flow rate of 20 μl/min. All experiments were performed in duplicate. Data transformation of the primary sensograms and overlay plots were prepared with BIAevaluation 3.2 software (BIACORE AB). The response from the reference surface was subtracted from that of each of the experimental surfaces to correct for refractive index changes, matrix effects, non-specific binding, injection noise and baseline drift [14]. The apparent stoichiometry of the surface complex (the averages number of moles of S-tagged VEGF or Hu-VEGF bound per mole of corresponded S-protein) was estimated from the saturating binding capacity of the surface and known molecular weights for the proteins according to manufacturer's instructions assuming them to be either 100% monomeric or 100% dimeric. Steady-state analysis of binding of Hu-VEGF or S-tagged VEGF to the corresponding immobilized S-protein was done in terms of a 'one-to-one interaction' model using BIAevaluation 3.2 software.

2.11. Polyethylenimine (PEI) conjugates

The conjugation procedure was described previously [2]. Briefly, 5 mM linear 25 kDa PEI (Polysciences Inc., Warrington, PA) was modified with 5 mM Traut's reagent (Pierce) in 50 mM triethanolamine, 0.15 M NaCl, 1 mM EDTA, pH 8.0 under argon for 20 min, while 0.66 mM HuS (or Hu-VEGF) was modified with 1.32 mM sulfo-MBS (Pierce Biothechnology) in conjugation buffer (0.1 M NaPi, 0.15 M NaCl, pH 7.2) for 30 min. Prior to modification, Hu-VEGF was concentrated on 10 K Microsep Centrufugal Device (Pall Life Sciences, Ann Arbor, MI) for 4 h at 4 °C. Modified HuS (or Hu-VEGF) and PEI were mixed separately at the molar ratio of 1:1 in conjugation buffer, and incubated for 4 h at room temperature. The conjugates were then purified by gel-filtration on SE40/100 (BioRad Laboratories, Hercules, CA). Protein concentration in conjugate preparations were determined by RP-HPLC on C_{18} Waters Nova-Pack 5 μm column as described under Protein refolding and purification. The pGL3 plasmid DNA (Promega Corporation, Madison, WI) encoding firefly luciferase was used for formation of DNA delivery complexes and for DNA delivery in tissue culture. The sizes and zeta-potentials of DNA delivery complexes were measured on DELSA 440SX (Beckman Coulter, Santa Ana, CA, USA) according to manufacturer's instructions. Zeta-potential for each sample was recorded at four angles: 8.9°, 17.6°, 26.3°, 35.2°, and averaged for each data set. Particle size readings were recorded at two angles: 26.3° and 35.2°, at both 16% and 84% stationary levels, and averaged for each data set. The DELSA and its sample cell were cleaned and calibrated before use.

The stationary levels were calibrated before every measurement.

3. Results

3.1. Expression of VEGF fused to a human docking tag

To develop a docking tag/adapter system based on human RNase I, we have constructed the pET29/Hu-tag vector for bacterial expression of recombinant proteins with the N-terminal 1–15 aa fragment of human RNase I (Hu-tag). The pET29/Hu-tag is a derivative of the pET-29a(+) vector containing human Hu-tag instead of bovine S-tag. The human $VEGF_{121}$ was cloned in the pET29/Hu-tag vector and expressed in *E. coli* strain BL21(DE3). The resulting recombinant protein comprising a 1–15 aa RNase I fragment, a 9-aa peptide linker, and 3-121 aa of human $VEGF_{121}$ was designated Hu-VEGF. It was purified from inclusion bodies with a final yield of 5–7 mg/l. Functional activity of Hu-VEGF was tested in VEGFR-2 autophosphorylation assay, and found to be comparable to the activity of the commercially available recombinant human $VEGF_{165}$ (R&D Systems, Minneapolis, MN) (Fig. 2A).

Hu-peptide differs from a corresponding fragment of bovine RNase A, S-peptide, in four positions (Fig. 2B). However, the key residues ^{8}phe, ^{11}gln, ^{13}met crucial for interactions of bovine S-peptide with S-protein, are conserved in Hu-peptide and therefore, Hu-tag, similarly to bovine S-tag, can form enzymatically active complexes with bovine S-protein [6,7]. Indeed, we found that a heterologous bovine S-protein/Hu-VEGF mixtures displayed ribonuclease activity at low nanomolar concentrations (Fig. 2B). Interestingly, S-tagged VEGF [2] containing bovine S-peptide displayed significantly lower activity in this assay (Fig. 2B). The ability of Hu-VEGF to interact with bovine S-protein provides an opportunity to use the great variety of S-protein based reagents developed for quantitation, blot detection, purification and precipitation of S-tagged proteins [15]. For example, we precipitated cellular VEGFR-2 using Hu-VEGF bound to S-protein agarose (Fig. 2C). Apparently, a 9-aa linker between Hu-tag and

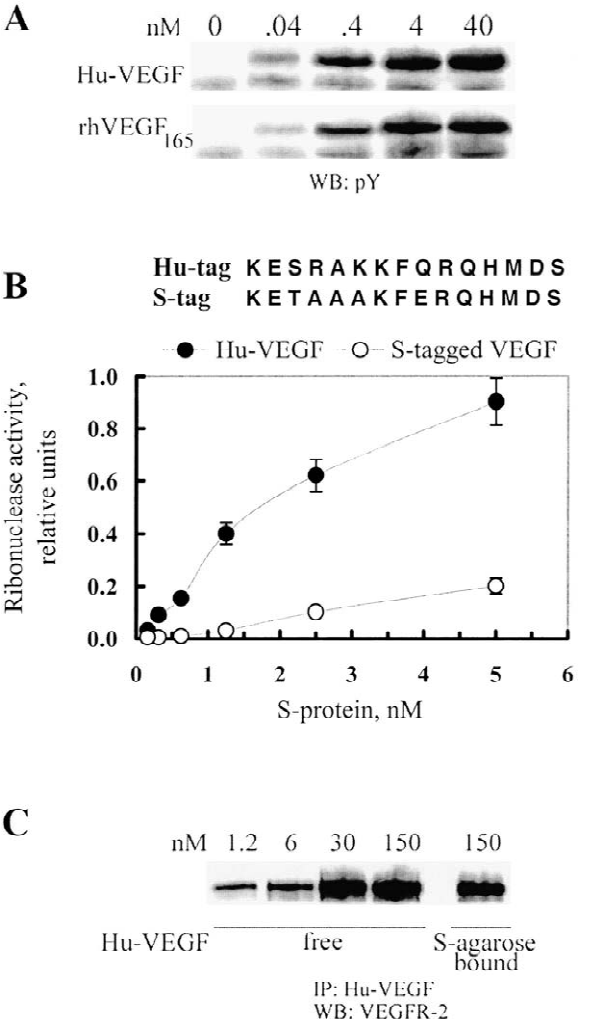

Fig. 2. Recombinant Hu-VEGF is functionally active. (A) Hu-VEGF activates VEGFR-2. After overnight starvation in DMEM with 0.5% FBS, near-confluent 293/KDR cells were shifted to serum-free DMEM with 0.5 mM sodium vanadate for 5 min at 37 °C. Cells were stimulated with Hu-VEGF or recombinant human $VEGF_{165}$ (R&D Systems) for 5 min at 37 °C; then lysed and analyzed by Western blotting using anti-phosphotyrosine RC20:HRPO conjugate (BD Transduction Labs, San Diego, CA). (B) Compexes of bovine S-protein with Hu-VEGF or S-tagged VEGF restore ribonuclease activity. One optical unit of acid-soluble material released from poly (C) incubated with S-protein complexes is defined as one relative unit of ribonuclease activity. (C) S-protein agarose bound Hu-VEGF retains its functional activity. VEGFR-2 was precipitated from clarified lysates of 293/KDR cells with free or S-agarose bound Hu-VEGF and analyzed by Western blotting.

VEGF allows docking of such a bulky payload as S-protein agarose without affecting VEGF targeting function, e.g. its ability to interact with VEGFR-2.

3.2. Construction of human recombinant S-protein

Bovine S-protein is obtained from bovine RNase A by limited digestion of RNase A with bacterial serine protease subtilisin [16]. The corresponding sequence in human RNase I is not susceptible to selective subtilisin cleavage [4]. Therefore we designed, expressed and purified human recombinant S-protein (HuS). In our strategy, the 1–15 aa fragment of RNase I is utilized as a docking tag in targeting proteins. Therefore, an RNase I fragment that interacts with Hu-tag might start at ^{16}asp (see, Table 1). However, we recently reported that the level of bacterial expression of bovine S-proteins is dramatically influenced by the nature of the N-terminal amino acid residues [8]. Therefore, apart from the HuS starting with ^{16}asp, we have also designed four HuS proteins with different N-termini (Table 1). The designing strategy included different starting points and introduction of either the ^{20}ser→ala, or the ^{19}pro→ala and ^{20}ser→ala substitutions into the N-terminus of HuS. The latter amino acid substitutions were designed to reconstitute the five N-terminal amino acids of the 18–124-aa bovine S-protein that was successfully expressed in a bacterial system [8]. All ORFs were cloned in pETBlue-1 and tested for inducible expression in *E. coli* strain Tuner(DE3)pLacI. Out of five constructs, only a protein with the ^{19}pro→ala and ^{20}ser→ala substitutions was found in induced bacterial lysates (data not shown). The protein was designated $^{18-125}$HuS and expressed in *E. coli* strain OrigamiB(DE3)pLacI. For large-scale expression, $^{18-125}$HuS was extended with two RNase I native C-terminal amino acids (^{126}asp and ^{127}ser), and sub-cloned in pET29a(+) bacterial expression vector. The resulting protein was designated $^{18-127}$HuS and expressed in *E. coli* strain BL21(DE3). The yield of $^{18-125}$HuS expressed in OrigamiB(DE3)pLacI was 12–14 mg/l, while expression of $^{18-127}$HuS in BL21(DE3) yielded 80 mg/l. Both HuS proteins were solubilized from inclusion bodies, refolded in the presence of 2-fold molar excess of Hu-peptide, and purified via a combination of cation-exchange chromatography and RP-HPLC. Although Hu-peptide was removed during RP-HPLC, both purified proteins retained the ability to bind Hu-peptide with concomitant reconstitution of ribonuclease activity. In contrast, HuS proteins refolded in the absence of Hu-peptide did not reconstitute ribonuclease activity (data not shown). Reconstituted ribonuclease activity was measured using the original Kunitz's assay [11] and a modified method of Libonati and Floridi [12] and compared to the activities of recombinant human RNase I and native bovine RNase A. We found that recombinant HuS/Hu-peptide complexes and recombinant RNase I displayed similar activities under both conditions (Table 2). In agreement with D'Alessio et al. [5], native and reconstituted human RNases were more active at pH 7.5, while bovine RNase A was more active at pH 5.

3.3. HuS/Hu-VEGF binding

In order to characterize affinity of HuS to Hu-VEGF and Hu-peptide, we measured the reconsti-

Table 1
Sense primers used for amplification of HuS ORFs with varying N-termini

	Human RNase I (partial amino acid sequence)													
	16 asp	17 ser	18 ser	19 pro	20 ser	21 ser	22 ser	23 ser	24 thr	25 tyr	26 cys	27 asn	28 gln	
Mutations	Sense primer													Protein
–	GAC	TCG	AGC	CCG	TCT	TCT	TCT							–
^{19}pro, ^{20}ser→ala			AGC	***GCT***	***GCC***	TCT	TCT	TCT	ACG	TAC	TGC	AAC	CAG	+
–				CCG	TCT	TCT	TCT	TCT	ACG	TAC	TGC			–
^{20}ser→ala					***GCT***	TCT	TCT	TCT	ACG	TAC	TGC	AAC	CAG	–
–						TCT	TCT	TCT	ACG	TAC	TGC	AAC	CAG	–

Table 2
Specific ribonuclease activity on different substrates (Kunitz units, U/mg)

	Substrate	
	yeast RNA (pH 5.0)	poly C (pH 7.5)
HuS/S-peptide	6	2000
RNase I	10	2200
RNAse A	56	210

tuted ribonuclease activity in HuS/Hu-VEGF and HuS/Hu-peptide mixtures under conditions of equilibrium between free and bound HuS (Fig. 3A, B). To derive equilibrium dissociation constant (K_D) values for corresponding complexes, the experimental data were analyzed with DYNAFIT software [10] with the assumption that the initial rate of the hydrolysis is proportional to the concentration of reconstituted ribonuclease [8]. We found that HuS protein binds Hu-peptide and Hu-VEGF with similar affinities (K_D of 110±23 and 162±16 nM, respectively). Both $^{18-125}$HuS and $^{18-127}$HuS proteins were tested in this assay, and were found to have the same affinities to human Hu-peptide and Hu-VEGF (data not shown).

3.4. Surface plasmon resonance analysis

To further characterize interactions between HuS and Hu-VEGF, we employed SPR analysis. Experimental conditions were established for the bovine system using bovine S-protein and S-tagged VEGF. The kinetics of association of 1 μM S-tagged VEGF to bovine S-protein immobilized on CM-5 chip surface (~300 RU) did not depend on a flow rate in the range from 2 to 75 μl/min (data not shown), indicating that mass transfer effects did not contribute to the observed protein binding [14]. A 10-fold excess of S-protein in the solution, but not a similar excess of bovine serum albumin, completely inhibited binding of S-tagged VEGF to the immobilized S-protein (Fig. 4A), indicating that specific S-tagged VEGF/S-protein interactions are responsible for SPR effects. The initial rates and the levels of binding of S-tagged VEGF to S-protein were dose-dependent and approached saturation at high S-tagged VEGF concentrations (Fig. 4B). Assuming that 100% of immobilized S-protein was active and

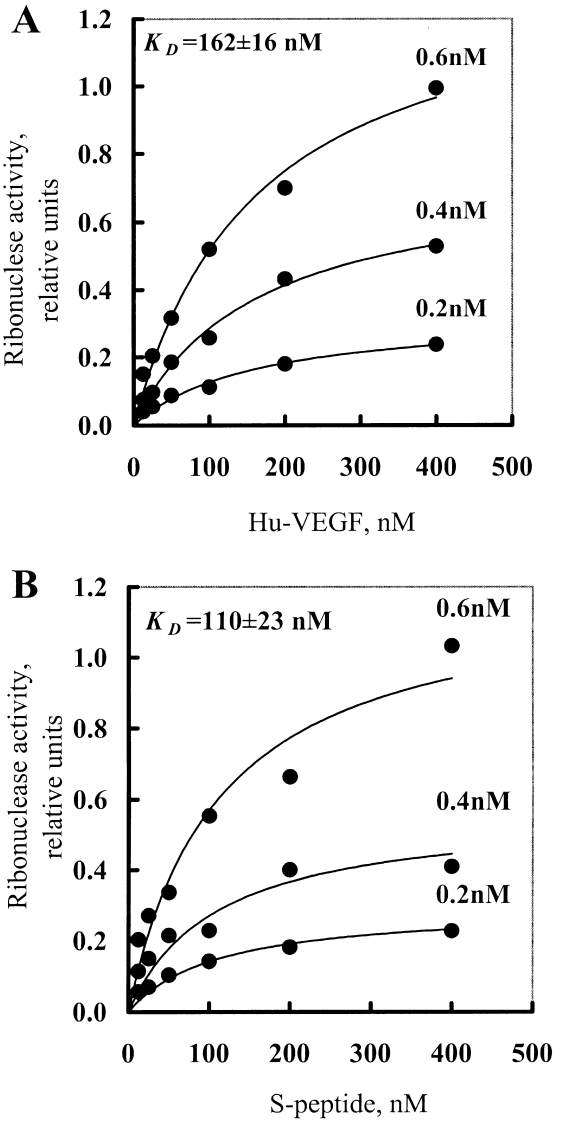

Fig. 3. Recombinant HuS forms similarly active complexes with Hu-VEGF and Hu-peptide. HuS at final concentrations of 0.2, 0.4 or 0.6 nM was mixed with varying amounts of Hu-VEGF (A) or Hu-peptide (B) in reaction buffer containing poly (C) substrate. The DYNAFIT software was used for calculation of the K_D values [10].

that 100% S-tagged VEGF molecules were either dimers or monomers, we calculated that the stoichiometry of binding at the saturating concentrations was, respectively, 0.15 and 0.3 moles of S-tagged VEGF per mole of S-protein. Dissociation of S-

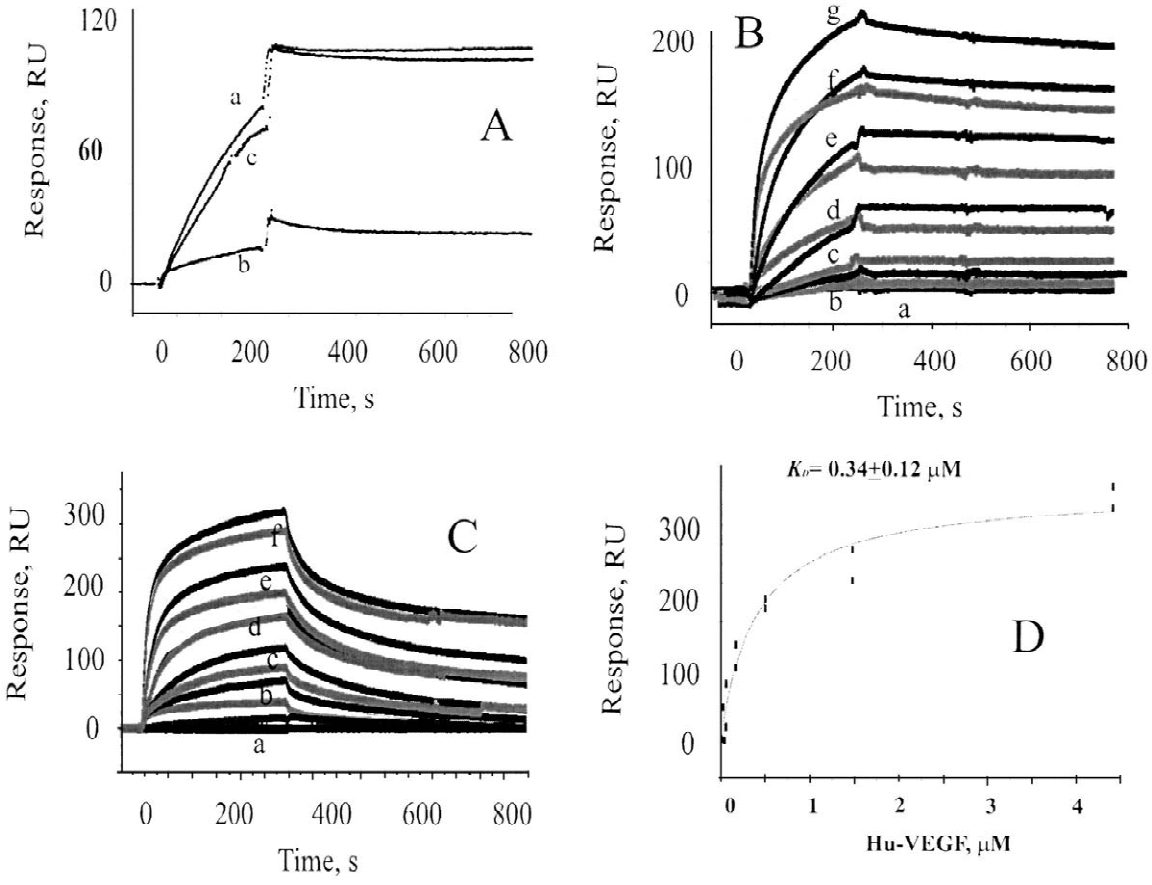

Fig. 4. Surface plasmon resonance analysis. (A) Competitive inhibition of S-tagged VEGF binding to CM5 chip surface with immobilized bovine S-protein. Overlay sensogram plots of 1 μM S-tagged VEGF injected at 2 μl/min over a sensor chip surface to which ~300 RU of S-protein was immobilized in the absence (a) and presence (b) of 10 μM of S-protein or 10 μM BSA (c). (B) Kinetic response data for S-tagged VEGF binding to CM5 chip surface with immobilized bovine S-protein. Overlay sensogram plots represent two repeated 10-μl injections of each protein concentration (14 nM, 41 nM, 124 nM, 370 nM, 1.11 μM, 3.33 μM, and 10.0. μM, a, b, c, d, e, f, and g, respectively), at 2 μl/min over a sensor chip surface with ~300 RU of immobilized S-protein. (C) Kinetic response data for Hu-VEGF binding to CM5 chip surface with immobilized $^{18-125}$HuS. Overlay sensogram plots represent two repeated 10-μl injections of each protein concentration (18 nM, 54 nM, 163 nM, 490 nM, 1.47 μM, and 4.4. μM, a, b, c, d, e, and f, respectively) at 2 μl/min over a sensor chip surface with ~380 RU of immobilized $^{18-125}$HuS. (D) Steady-state analysis of Hu-VEGF with $^{18-125}$HuS interactions. Steady-state data (squares) from the sensograms shown on Fig. 4C. Solid line is simulated based on the 'one-to-one interaction' model and best-fit parameters R_{max} (the maximal response) = 309±28 RU and K_D = 340±120 nM.

tagged VEGF was very slow. The low rate of this process could not be attributed to the strong rebinding of dissociated S-tagged VEGF because coinjection of 10 or 50 μM S-protein at the dissociation step did not accelerate dissociation (data not shown).

Serial injections of Hu-VEGF over the sensor chip surface with immobilized $^{18-125}$HuS (Fig. 4C) revealed the same concentration dependent manner of binding and tendency to saturation. Assuming that 100% of immobilized HuS was active and that 100% Hu-VEGF molecules were either dimers or monomers, we calculated that the stoichiometry of binding at the saturating concentrations was, respectively, 0.22 and 0.45 moles of Hu-VEGF per mole of HuS. We found a detectable dissociation of ~50% of bound Hu-VEGF, suggesting that two fractions of

complex with different stability might exist. The average K_D value of ~340±120 nM could be roughly estimated from the levels of steady-state responses (Fig. 4D).

3.5. HuS/Hu-VEGF based gene delivery complex

To obtain a proof-of-principle for the utility of the HuS/Hu-tag docking system for targeted drug delivery, we assembled Hu-VEGF based gene delivery complexes. As a DNA carrier we used polyethylenimine (PEI), a well-known DNA binding and condensing agent [17]. To compare DNA delivery by complexes based on a docking system vs. direct VEGF conjugation, we prepared two types of conjugates: PEI–HuS and PEI–Hu-VEGF, both at the same molar ratio of 1:1. We found that purified PEI–Hu-VEGF conjugate was less efficient in induction of VEGFR-2 tyrosine autophosphorylation than similarly treated Hu-VEGF (Fig. 5A). Although tyrosine phosphorylation reached plateaus at the same Hu-VEGF concentrations, the level of tyrosine phosphorylation for PEI–Hu-VEGF was significantly lower than that for Hu-VEGF.

Purified PEI–HuS was docked to Hu-VEGF to form a non-covalent PEI–HuS/Hu-VEGF complex, and then both PEI–HuS/Hu-VEGF complex and PEI–Hu-VEGF conjugate were loaded with the pGL3 plasmid DNA for mammalian expression of firefly luciferase. The resulting targeting complexes were analyzed by dynamic light scattering to select the N/P ratio (where N is the number of PEI amino groups, and P is the number of DNA phosphate groups) that provides for negative zeta-potentials and the smallest complex size. Negative zeta-potential of targeting complexes is critical for reducing non-specific binding to negatively charged cell surface, while the small size of the complexes would be beneficial for DNA delivery in vivo. We found that PEI–protein conjugates formed complexes with negative zeta-potentials at significantly higher N/P ratios compared with free PEI (Fig. 5B). Interestingly, despite similar negative zeta-potentials at the N/P ratio of 3, only PEI–HuS/Hu-VEGF formed relatively compact 200 nm complexes, while sizes of the other complexes varied from 0.5 to 1.5 μm (Fig. 5C). PEI–HuS/Hu-VEGF and PEI–Hu-VEGF based gene delivery complexes formulated at the N/P ratio of 3 were tested on 293/KDR cells. Parental HEK293 cells lacking VEGFR-2 served as controls for non-specific DNA delivery, since previous experiments indicated that 293/KDR and HEK293 cells are similarly susceptible to gene delivery by untargeted PEI/DNA complexes [2,3]. Judging by a 25-fold higher level of luciferase expression in 293/KDR vs. HEK293 cells, VEGF-driven assembled complexes delivered DNA via VEGFR-2 mediated process (Fig. 5D). DNA delivery by the PEI–Hu-VEGF driven complexes resulted in significantly lower levels of luciferase expression (Fig. 5D).

4. Discussion

Here we report the development of a fully humanized docking system for assembly of complexes for targeted drug delivery. The docking system is based on high affinity interaction of two fragments of human RNase I, Hu-peptide and HuS protein. To validate the humanized docking system, we have used VEGF as a targeting protein for receptor-mediated DNA delivery. We have recently reported that VEGF-based drug delivery preferentially targets cells overexpressing VEGFR-2 [2,18]. Since these cells are expected to be present at the sites of pathological angiogenesis (see, for example Refs. [19–21]), the VEGF-driven drug delivery vehicles based on a humanized docking system might be developed into anti-angiogenic therapeutics. Fusion of Hu-peptide to $VEGF_{121}$ does not affect its folding, as judged by interactions with its receptor, VEGFR-2 (Fig. 2A). Importantly, Hu-VEGF bound to S-protein agarose retains the ability to bind and precipitate cellular VEGFR-2, suggesting that a 9-aa peptide linker between Hu-tag and VEGF will allow docking of bulky payload modules without destroying the VEGF targeting function (Fig. 2C).

To develop a human adapter protein, HuS, we have constructed five versions of this protein with different N-terminal amino acid residues. These efforts were based on our findings that the level of expression of the corresponding bovine S-protein crucially depended on the nature of the N-terminal amino acids [8]. Indeed, we found a detectable expression of $^{18-125}$HuS only after reconstitution of

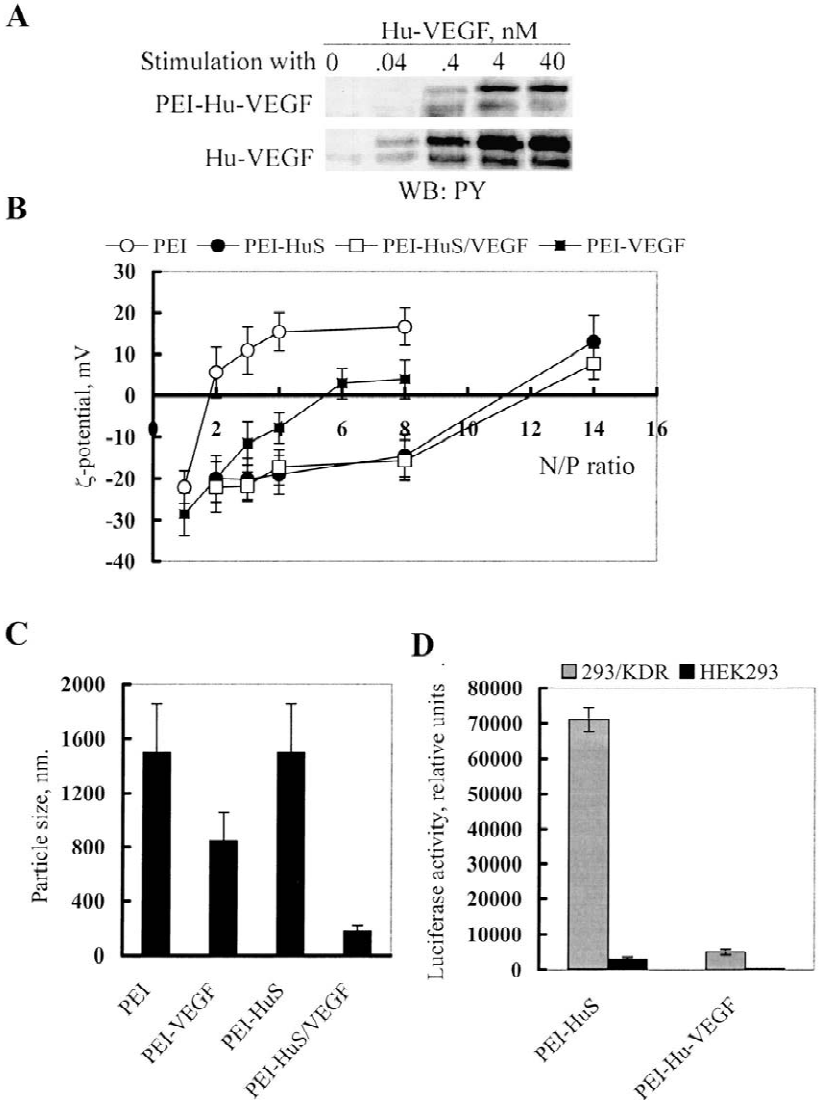

Fig. 5. DNA delivery module assembly on Hu-VEGF is more efficient than its direct cross-linking to Hu-VEGF. (A) Direct PEI crosslinking affects functional activity of Hu-VEGF. VEGFR-2 tyrosine autophosphorylation assay was done as described in legend for Fig. 2A. (B) Zeta-potentials of DNA delivery complexes. To assemble PEI–HuS/Hu-VEGF complex, PEI–HuS was mixed with Hu-VEGF at the HuS to Hu-VEGF ratio of 1.5:1 in 5% glucose. The same amounts of glucose were added separately to PEI–Hu-VEGF, PEI–HuS, and free PEI. All four mixtures were incubated on ice for 20 min, then diluted with 5% glucose to final PEI concentrations of 3 μM, and mixed separately with DNA to form complexes with varying N/P ratios. After 20-min incubations on ice, the samples were used for light scattering measurements. (C) Complex assembly and loading with DNA at $N/P = 3$ was done as described in legend for Fig. 5B. (D) Targeted DNA delivery. Twenty-four hours before the experiment, HEK293 and 293/KDR cells were plated on 24-well plates at densities of 10^4 cells/well. Complex assembly and loading with DNA at $N/P = 3$ was done as described in legend for Fig. 5B. After 20-min incubations on ice, the complexes were added to cells in complete culture medium to final concentrations of 5 nM Hu-VEGF,32 nM PEI–HuS and 1 μg DNA per well. Cells from triplicate wells were lyzed and assayed for luciferase activity (Bright-Glo™ Luciferase Assay System, Promega) 48 h after DNA delivery. The DNA delivery experiments were repeated twice.

the first five amino acid residues of bovine S-protein via the ^{19}pro→ala and ^{20}ser→ala substitutions (Table 1). The crucial role of N-terminal amino acid residues for efficiency of bacterial protein expression is well established and original findings are summarized in the 'N-end rule' [22]. Surprisingly, failed variants of HuS start with amino acid residues permissible under the 'N-end rule', suggesting more complex regulatory mechanisms. It should be noted that the ^{19}pro→ala and ^{20}ser→ala substitutions in HuS, as well as the presence of the 9-aa linker in Hu-VEGF, might provoke immune response in humans. In this case, development of unmodified HuS and use of accepted $(gly_4ser)_n$ linkers will be necessary for human use of our docking system.

Bacterially expressed HuS was refolded in the presence of Hu-peptide, which was subsequently removed from the protein preparations by RP-HPLC. This protocol resulted in a functionally active HuS that is capable of reconstituting ribonuclease activity upon binding Hu-peptide or S-peptide. Efficiency of the refolding procedure chosen for HuS was confirmed by the fact that ribonuclease activity of HuS/Hu-peptide complexes in Kunitz assay was close to that of intact recombinant RNase I (Table 2). HuS refolded in the absence of Hu-peptide was functionally inactive, indicating that the presence of Hu-peptide during refolding is necessary for proper positioning of eight cys residues that form four disulfide bonds in RNase I.

Binding HuS to Hu-VEGF was characterized indirectly, by analysis of enzymatic activity, and directly, by using plasmon surface resonance. Both techniques yielded K_D in the submicromolar range (Figs. 3 and 4), or approximately 10-fold higher than K_D values for complexes of bovine S-protein with S-tagged VEGF [8]. However, it is not known whether these differences in K_D values reflect the difference in stability of the respective complexes. Indeed, binding of S-peptide to S-protein involves formation of an initiation complex, followed by conformation transitions in both S-peptide and S-protein that result in formation of a more stable complex [23]. Assuming that similar processes take place upon interactions between HuS and Hu-VEGF, it will require additional studies to characterize the stability of these complexes. In this respect, it is interesting that dissociation kinetics observed in surface plasmon resonance experiments suggest the existence of complexes with different stability (Fig. 4C). Since stability of these complexes might determine their utility for targeted drug delivery, further characterization of the HuS/Hu-peptide interaction is now in progress.

To test the humanized docking system, we have constructed a payload module for nucleic acid delivery, PEI–HuS. We found that PEI–HuS/Hu-VEGF complexes efficiently deliver DNA into cells via VEGFR-2 mediated process (Fig. 5D). In contrast, complexes based on Hu-VEGF directly modified with PEI were significantly less efficient (Fig. 5D). These results are not particularly surprising, since chemical modifications of targeting proteins usually interfere with their target binding [1]. In this particular case, Hu-VEGF crosslinked to PEI was significantly less effective in activation of VEGFR-2 than unmodified Hu-VEGF (Fig. 5A).

Taken together, our data indicates that a docking system based on interactions between fragments of human RNase I can be used for construction of assembled targeting complexes. Importantly, unlike several other RNases, human RNase I is not cytotoxic even at micromolar concentrations, and therefore might be used in complexes for delivery of beneficial as well as toxic payloads [24,25]. Experiments are in progress to test several humanized payload modules for targeted delivery in vivo.

Acknowledgements

This work was supported in part by a grant from National Institutes of Health (# 2R44 HL6143-02).

References

[1] G.M. Dubowchik, M.A. Walker, Receptor-mediated and enzyme-dependent targeting of cytotoxic anticancer drugs, Pharmacol. Ther. 83 (1999) 67–123.
[2] M.V. Backer, R. Aloise, K. Przekop, K. Stoletov, J.M. Backer, Molecular vehicles for targeted drug delivery, Bioconj. Chem. 13 (2002) 462–467.
[3] E.K. Gaidamakova, M.V. Backer, J.M. Backer, Molecular vehicle for target-mediated delivery of therapeutic and diagnostics, J. Controlled Release 74 (2001) 341–347.
[4] J. Pous, G. Mallorquí-Fernández, R. Peracaula, S.S. Terzyan,

J. Futami, H. Tada, H. Yamada, M. Seno, R. de Llorens, F.X. Gomis-Rüth, M. Coll, Three-dimensional structure of human RNase 1 delta N7 at 1.9 A resolution, Acta Crystallogr. D. Biol. Crystallogr. 57 (2001) 498–505.

[5] G. D'Alessio, J.F. Riordan, Ribonucleases: Structures and Functions, Academic Press, New York, 1997.

[6] P.R. Connelly, R. Varadarajan, J.M. Sturtevant, F.M. Richards, Thermodynamics of protein–peptide interactions in the ribonuclease S system studied by titration calorimetry, Biochemistry 29 (1990) 6108–6114.

[7] S. Dubel, Reconstitution of human pancreatic RNase from two separate fragments fused to different single chain antibody fragments: on the way to binary immunotoxins, Tumor Target. 4 (1999) 37–46.

[8] M.V. Backer, T.I. Gaynutdinov, R. Aloise, K. Przekop, J.M. Backer, Engineering S-protein fragments of bovine ribonuclease A for targeted drug delivery, Prot. Exp. Purif. 26 (2002) 455–461.

[9] M.V. Backer, J.M. Backer, Functionally active VEGF fusion proteins, Prot. Exp. Purif. 23 (2001) 1–7.

[10] P. Kuzmic, Program DYNAFIT for the analysis of enzyme kinetic data: Application to HIV proteinase, Anal. Biochem. 237 (1996) 260–273.

[11] M. Kunitz, A spectrophotometric method for the measurement of ribonuclease activity, J. Biol. Chem. 164 (1946) 563–568.

[12] M. Libonati, A. Floridi, Breakdown of double-stranded RNA by bull semen ribonuclease, Eur. J. Biochem. 8 (1969) 81–87.

[13] I.I. Gorshkova, J.W. Rausch, S.F. Le Grice, R.J. Crouch, HIV-1 reverse transcriptase interaction with model RNA–DNA duplexes, Anal. Biochem. 291 (2001) 198–206.

[14] T.A. Morton, D.G. Myzska, Methods in Enzymology, Kinetic Analysis of Macromolecular Interactions Using Surface Plasmon Resonance Biosensors, Part B, Academic Press, New York, 1998, pp. 268–294.

[15] M. McCormic, R. Mierendorf, S-tag: a multipurpose fusion peptide for recombinant proteins, inNovations, Novagen Bull. 13 (2001) 4–6.

[16] F.M. Richards, P.J. Vithayathil, The preparation of subtilisin-modified ribonuclease and the separation of the peptide and protein components, J. Biol. Chem. 234 (1959) 1459–1465.

[17] O. Boussif, F. Lezoualch, M.-A. Zanta, M.D. Mergny, D. Scherman, B. Demeneix, J.-P. Behr, A versatile vector for gene and oligonucleotide transfer into cells in culture and in vivo, Proc. Natl. Acad. Sci. USA 92 (1995) 7297–7301.

[18] M.V. Backer, J.M. Backer, Targeting endothelial cells overexpressing VEGFR-2: selective toxicity of Shiga-like toxin-VEGF fusion proteins, Bioconjugate Chem. 12 (2001) 1066–1073.

[19] L.F. Brown, B. Berse, R.W. Jackman, K. Tognazzi, E.J. Manseau, H.F. Dvorak, D.R. Senger, Increased expression of vascular permeability factor (vascular endothelial growth factor) and its receptors in kidney and bladder carcinomas, Am. J. Pathol. 143 (1993) 1255–1262.

[20] K.H. Plate, G. Breier, B. Millauer, A. Ullrich, W. Risau, Up-regulation of vascular endothelial growth factor and its cognate receptors in a rat glioma model of tumor angiogenesis, Cancer Res. 53 (1993) 5822–5827.

[21] L.F. Brown, B. Berse, R.W. Jackman, K. Tognazzi, A.J. Guidi, H.F. Dvorak, D.R. Enger, J.L. Connolly, S.J. Schnitt, Expression of vascular permeability factor (vascular endothelial growth factor) and its receptors in breast cancer, Hum. Pathol. 26 (1995) 86–91.

[22] J.W. Tobias, T.E. Shrader, G. Rocap, A. Varchavsky, The N-end rule in bacteria, Science 254 (1991) 1374–1377.

[23] J.M. Goldberg, R.L. Baldwin, A specific transition state for S-peptide combining with folded S-protein and then refolding, Proc. Natl. Acad. Sci. USA 96 (1999) 2019–2024.

[24] R.T. Raines, Ribonuclease A, Chem. Rev. 98 (1998) 1045–1065.

[25] J. Futami, M. Seno, M. Ueda, H. Tada, H. Yamada, Inhibition of cell growth by a fused protein of human ribonuclease 1 and human basic fibroblast growth factor, Prot. Eng. 12 (1999) 1013–1019.